International Journal of Mechanical, Industrial and Aerospace Sciences
ISSN: 2517-9950
Vol:6, No:10, 2012

Modeling and Implementation of an Oceanic-Robot Glider

C. Clements, M. Hasenohr, and A. Anvar

***Abstract*—**A glider is in essence an unpowered vehicle and in this project we designed and built an oceanic glider, designed to operate underwater. This Glider was designed to collect ocean data such as temperature, pressure and (in future measures physical dimensions of the operating environment) and output this data to an external source. Development of the Oceanic Glider required research into various actuation systems that control buoyancy, pitch and yaw and the dynamics of these systems. It also involved the design and manufacture of the Glider and the design and implementation of a controller that enabled the Glider to navigate and move in an appropriate manner.

***Keywords*—**Ocean Glider, Robot, Automation, Command, Control, Navigation.

I. Introduction

THE Oceanic Glider is an unmanned, autonomous underwater vehicle (AUV) that is propelled using unconventional methods. The concept behind the Oceanic Glider's operation involves several systems. Motion is achieved by employing a ballast system to inject and expel water, changing the Glider's weight and allowing it to ascend and descend in the vertical plane. This vertical motion is coupled with a sliding mass, which moves about the Glider's centre of gravity, altering the Glider's pitch and creating an angle of attack. These two systems in conjunction with the Glider's fixed wings create lift and a component of this lift is in the horizontal plane, creating horizontal motion [1].

II. Motivation

The ocean comprises the largest percentage of the Earth's surface and has a diverse ecosystem, which mankind has a moral obligation to monitor and maintain. This maintenance requires a significant contribution in the form of human and vehicular resources, necessary to obtain adequate research data. It is proposed that the Oceanic Glider will fulfill this requirement and provide an alternative to both conventionally powered manned and unmanned craft. Oceanic gliders are well suited to this application as they do not require conventional fuel and therefore have a longer service life, up to a year or more, while covering thousands of kilometers [2].

C. Clements is a Graduate Engineer from the School of Mechanical Engineering, the University of Adelaide 5005 Australia.
M. Hasenohr is a Graduate Engineer from the School of Mechanical Engineering, the University of Adelaide 5005 Australia.
A. Anvar is with the School of Mechanical Engineering, the University of Adelaide 5005 AUSTRALIA (e-mail: amir.anvar@adelaide.edu.au).

III. Design Evolution

A fundamental part of the design process is the formation of concept designs. This is a systematic process involving the analysis of each individual subsystem of the Glider, resulting in the formation of several designs that fulfill the project goals. This enables the design that most comprehensively fulfils the requirements of the project to be selected and any possible flaws in the design to be identified and removed.
During the concept generation phase, focus was placed upon hydrodynamic performance and the reduction of manufacturing expenses. Computational Fluid Dynamics (CFD) analysis was performed for several concept designs which is displayed in Figure 1.

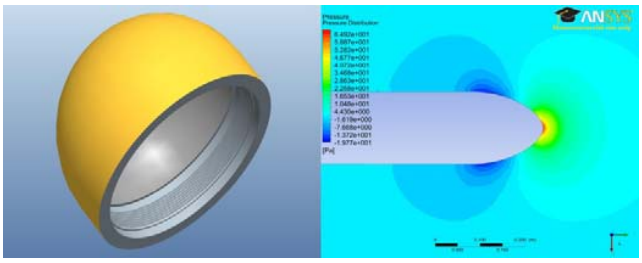

Fig. 1 Nose cone similar in design to the Slocum Glider

This first concept shown above is similar to that of the Slocum glider. This nose cone has a half spherical geometry and a relatively bluff design, which decreases the material related cost compared to following concepts. However, it is also the least hydrodynamic design, producing the highest drag due to the large stagnation pressure and pressure distribution associated with the bluff nose. The above figure illustrates that the stagnation point occurs at the very tip of the nose cone and the magnitude of this stagnation pressure is 64.92 Pa. It should also be noted that the minimum pressure value suggested by this analysis is negative, with a magnitude of -19.77 Pa. However, this pressure is relative to the reference pressure during the Glider's operation, which has a minimum of 1 atmosphere at the water's surface and increases with depth.

The second model illustrated in Figure 2 is similar to that of the Spray glider, and employs a compromise between hydrodynamics and simplicity. The above figure again illustrates that the stagnation point occurs at the very tip of the nose with a magnitude of 64.50 Pa, which is only a fraction smaller than the first concept. However the overall pressure distribution is also smaller in magnitude, implying a decrease in drag between the concepts. Again it should also be noted

that the minimum pressure value is negative only with respect to the reference operating pressure.

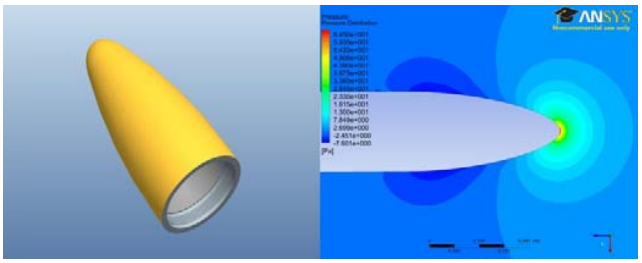

Fig. 2 Nose cone similar in design to the Spray Glider

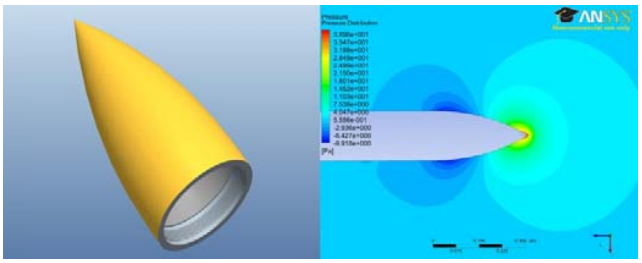

Fig. 3 Nose cone similar in design to the Sea-Glider

The third concept presented in Figure 3 is similar in design to that of the Sea-Glider. This is the most streamlined nose cone and has a length and maximum diameter identical to that of the second concept design and as a result has a similar material cost. Furthermore, this model also has the most hydrodynamic design, which is illustrated by the low stagnation pressure and associated pressure distribution. This stagnation pressure has a magnitude of 38.96 Pa, which is reduced by approximately 40% compared to the other concepts, resulting in a design that produces the least drag.

The wing assembly is a crucial element of the Oceanic Glider design, as the wings generate the lift force necessary to produce horizontal motion. Several concepts have been proposed, varying according to the considerations of lift generation, drag reduction and manufacturability.

One of the considerations in wing design was wing sweep, which is characterized by wings oriented at an angle other than 90 degrees from the fuselage or central body. The benefit of this wing configuration is the reduction of drag and shockwaves as the craft approaches transonic speeds. While the Oceanic Glider operates at considerably lower speeds, swept wings allow debris such as seaweed, which may build up over time to be dissipated by the flow

Wings have an airfoil profile and variations in this profile can drastically change the wing performance; consequently it is critical to select a suitable airfoil for the design. There are a multitude of airfoil shapes that have been published and amongst the most common are the NACA airfoils. Two suitable airfoils with differing geometry and performance have been selected and analysed below, namely the NACA 0012 and NACA 4412 airfoils.

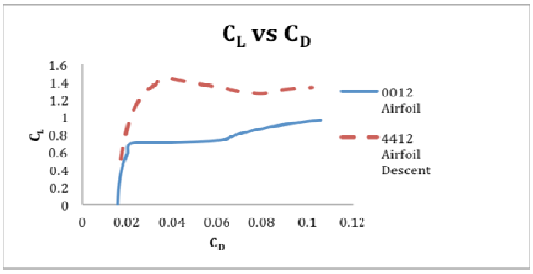

Fig. 4 CL verses CD plots for both airfoils descent

The trend of the above Figure 4 illustrates that the 4412 airfoil has a much higher lift coefficient when compared to the 0012 airfoil during descent. However, another consideration that must be made is the difference between the lift generated during ascent and descent, which would ideally be equal in both instances. This is not the case for cambered airfoils, which produce significantly less lift and subsequent horizontal velocity during ascent compared to descent. This is because during descent a low pressure region exists on the top surface of the wing compared to a high pressure region on the bottom surface of the wing. This pressure distribution is reversed during ascent and the below Figure 5 illustrates the effect of this reversal in conjunction with wing camber upon lift produced during the Glider's ascent:

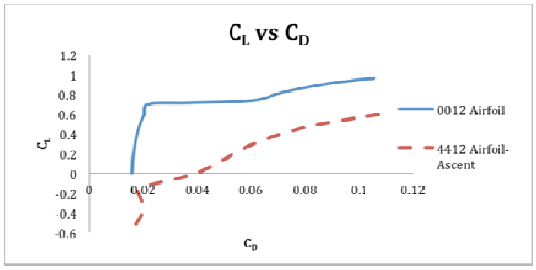

Fig. 5 Comparing L/D for the 0012 and 4412 Airfoil during ascent

This analysis indicates that the 4412 airfoil produces significantly more lift while descending compared to the 0012 profile, although this is reversed during ascent.

IV. Design Specification

Tables I and II summaries both the internal and external components of the Glider:

TABLE I
. Internal Components

Hull Length	1.1 m
Wing Span	1.1 m
Wing Chord	100 mm
Maximum Hull Diameter	161 mm
Microcontroller	Arduino Mega
Dead Reckoning	Atomic 6-dof IMU
Surface Navigation	Navman OEM GPS
Communications	UM-12 RF 433 MHz

TABLE II
EXTERNAL COMPONENTS

Pressure Sensor	10 bar absolute pressure sensor
Temperature Senor	LM35 sensor
Power Source	Sealed lead acid battery
Buoyancy System	2 gear pumps

It should be noted that in the future, more sensors could be incorporated into the design for oceanic underwater environmental survey and study.

V. AUTOMATION

The components described in the design specification all combine to form the overall control and automation system of the Oceanic Glider, which directly controls and actuates all of the Glider's systems and allows it to function autonomously. To facilitate the integration of these control systems, multi-level printed circuit boards (PCB's) were designed to easily connect and locate these systems together in a compact manner as shown in Figure 6.

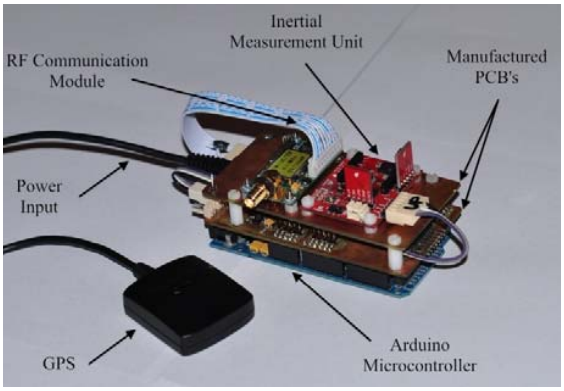

Fig. 6 Main Control Board

The Glider's automation can be separated into several different sections, namely navigation, communication and sensor payload. A control flow diagram detailing these systems and the manner in which they interact is displayed in Figure 7 with the inputs and outputs to and from the Arduino system at the top and bottom respectively.

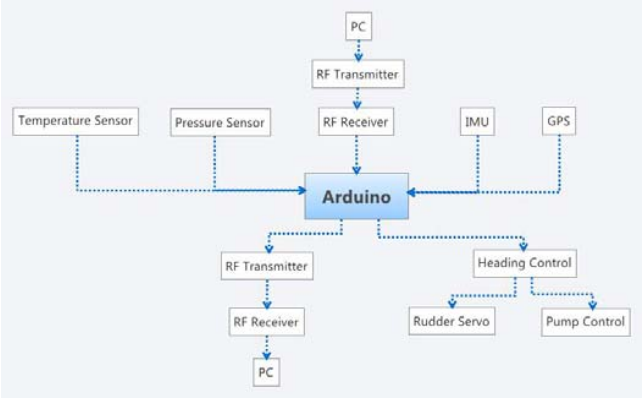

Fig. 7 Automation Control Flow Diagram

The navigation system has to both navigate heading and control the Glider's ascent and descent through the water column. The latter was controlled by the pump board, where depth was varied based upon an input from the main controller. This process occurs in several steps:

1. The pressure sensor outputs pressure values to the Arduino microcontroller.
2. These pressure values are then used by the Arduino to determine the depth of the Glider.
3. If the Glider is below or above specified depth a signal is sent to the pump board to activate the appropriate pump, causing the Glider to either descend or ascend based upon the pressure value.

The Glider's heading was controlled through the use of a rudder and servo, both mounted in the tail of the Glider. This servo actuates the rudder and receives its inputs from the GPS and Arduino systems. The GPS functions by automatically attaining a fix when at the surface and once this connection is made the Glider's location, heading and velocity are outputted to the Arduino [5]. To further describe the heading control system, consider the situation where the Glider is travelling from position 1 to position 2 as shown in Figure 8.

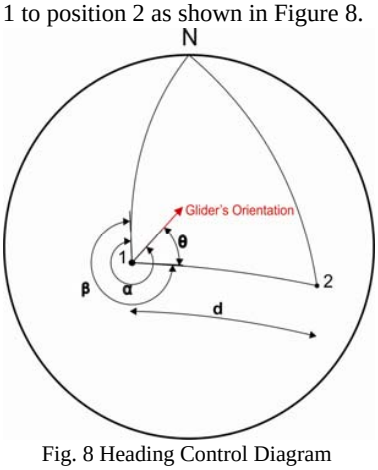

Fig. 8 Heading Control Diagram

Initially the distance between the two points d is calculated, which represents the distance the Glider is required to travel to complete its mission. This distance was calculated using the Haversine formula, which determines the distance between two points along the Earth's surface. This equation is described below:

$$h = sin^2\left(\frac{\Delta lat}{2}\right) + \cos(lat_1)\cos(lat_2)sin^2\left(\frac{\Delta long}{2}\right) \quad (1)$$

$$c = 2arctan^2\left(\frac{\sqrt{h}}{\sqrt{1-h}}\right) \quad (2)$$

$$d = Rc$$

lat_1 = latitude at position 1 in decimal degrees
lat_2 = latitude at position 2 in decimal degrees
Δlat = change in latitude between points 1 and 2
$\Delta long$= change in longitude between points 1 and 2
R = the radius of the Earth

Once this distance has been calculated, the Glider's bearing is determined. This involves resolving several angles, namely α and β which were displayed previously. Firstly, the forward azimuth angle α is calculated, which is achieved directly by the GPS once the Glider has surfaced and a fix is attained. The angle β is then determined with respect to the Glider's initial position and destination, using the equation below:

$$\beta = arctan^2\left(\frac{\sin(\Delta long)\cos(lat_2)}{\cos(lat_1)\sin(lat_2) - \sin(lat_1)\cos(lat_2)\cos(\Delta long)}\right) \quad (3)$$

The desired angle θ is then determined as the difference between the angles α and β and represents the angle the Glider is required to rotate such that it is oriented in the direction of its destination. This angle is then used to actuate the rudder servo based upon the magnitude θ (differs from 0º).

The communication system is used to coordinate the various Glider functions and transmit sampled data.

VI. Final Design Analysis

The final design was again analysed using CFD to estimate the lift and drag performance. Figure 9 displays the pressure distribution about the central plane of the Glider.

This figure clearly illustrates the high pressure on the top surface of the Glider compared to the low pressure on the bottom surface and this pressure distribution is the lift generated by the fuselage. The greater the magnitude of this pressure difference, the more lift is generated, and the general direction in which the lift acts is perpendicular to the longitudinal centerline of the Glider. Figure 10 also illustrates the high pressure at the nose of the Glider compared to the lower pressure at the tail, which is undesirable and manifests as drag.

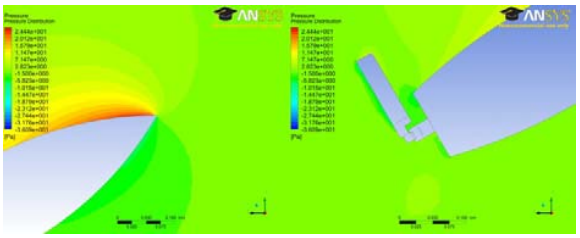

Fig. 9 Pressure Distribution

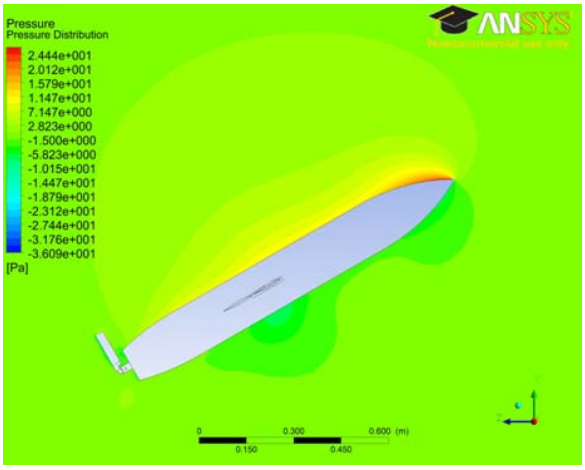

Fig. 10 CFD of high and low Pressure locations of surface body

The wings of the Glider also produce a large amount of lift, which has a similar orientation to the lift produced by the fuselage (see Figure 11).

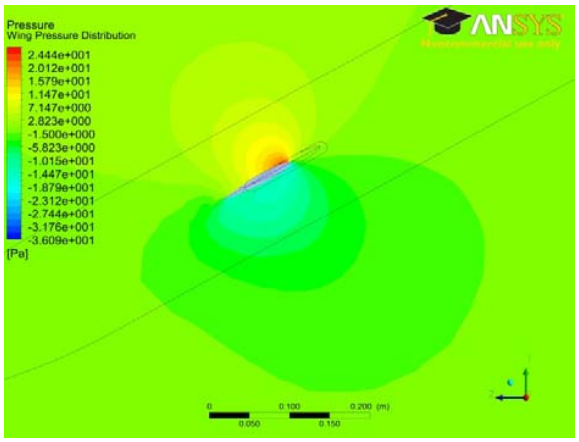

Fig.11 Wing Pressure Distribution

A. Dynamics

For the purposes of this project, the Glider's dynamics were modelled as a steady glide, which was assumed to be an equilibrium state. This is a reasonable assumption because the transitions and inflections between the two steady glide cases are gradual, simplifying the hydrodynamic effects [3]. The four main forces acting upon the Glider during its operation

are buoyancy, weight, lift and drag [4]. These forces were estimated using the following engineering equations.

$$F = \rho_f V_{disp} g \quad (4)$$

$$W = mg \quad (5)$$

$$L = \frac{1}{2}\rho_f \, C_L A_W V^2 \quad (6)$$

$$D = \frac{1}{2}\rho_f \, C_B A_B V^2 + \frac{1}{2}\rho_f \, C_W A_W V^2 \quad (7)$$

It should be noted that some of these parameters were estimated using various software packages and then verified using simplified analytical methods.

Figure 12 represent a free body diagram (FBD) displays the major forces discussed previously. It should be noted that some of these forces and angles are exaggerated for illustrative purposes and do not provide an accurate representation of magnitude or position. This figure also displays both the body-fixed coordinate system (with origin *o*) and the Earth-fixed coordinate system (with origin O).

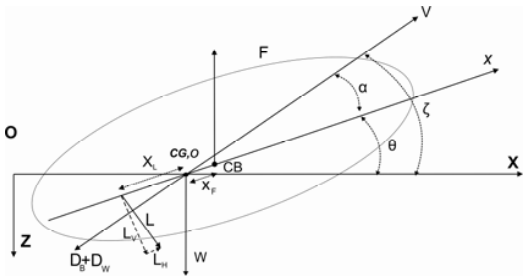

Fig. 12 Simplified FBD During Ascent

The terms in this FBD are presented in the table below:

TABLE III
FBD TERMS

CB	Centre of buoyancy	
CG	Centre of Gravity	
D_B	Drag due to Glider body	(N)
D_W	Drag due to Glider wings	(N)
L	Lift force	(N)
F	Buoyancy force	(N)
W	Weight force	(N)
V	Glider Velocity	(m/s)
x_G	*x*-distance from body-fixed origin to centre of gravity	(m)
x_F	*x*-distance from body fixed origin to centre of buoyancy	(m)
z_G	z-distance from body fixed origin to centre of gravity	(m)
(o,x,y,z)	Body-fixed coordinate system	
(O,X,Y,Z)	Earth-fixed coordinate system	
α	Angle of attack	°
θ	Pitch angle	°
ζ	Glide path angle ($\zeta = \theta + \alpha$)	°

VII. Testing and Results

Several tests have been undertaken using the Oceanic Glider at DSTO's testing facilities. These tests included buoyancy tests, sensor payload tests and operations tests

The buoyancy test involved submerging the Glider in a salt-water test tank and adding mass to the Glider until it reached a neutrally buoyant state. This resulted in a weight of 22.08 kg, which is very close to the predicted theoretical value of 22.68 kg. The neutrally buoyant mass is important for the operation of the Glider because the ballast system has to operate about this point to allow the Glider to ascend and descend and hence achieve motion. Figure 13 depicts the Glider in its neutrally buoyant state in equilibrium just below the surface:

Fig. 13 Buoyancy Test

The sensor payload test consisted of both a temperature sensor test, and pressure sensor test.

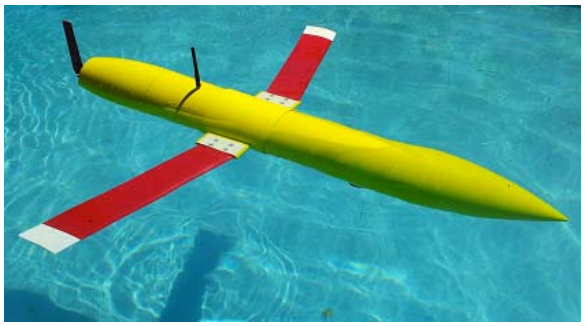

Fig. 14 Final Design

This test involved placing the Glider into the operations tank, where it was gradually lowered to a depth of 4 metres whilst data was being recorded (see Figure 14). Figures 15 and 16 illustrate the pressure and temperature data obtained from the payload test:

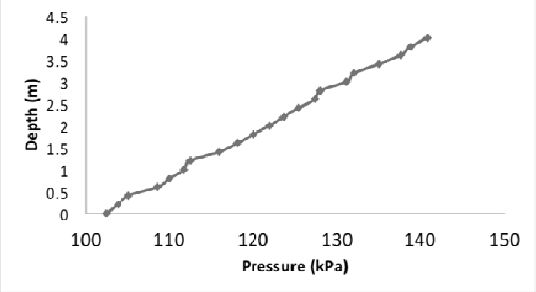

Fig.15 Pressure Data

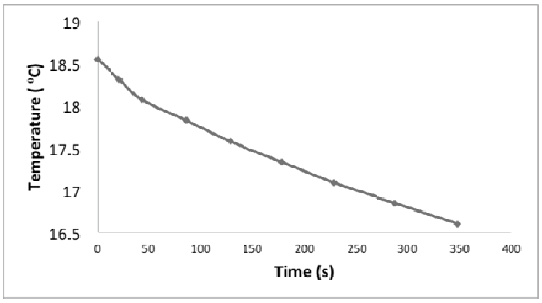

Fig. 16 Temperature Data

These results were as expected and followed the predicted theoretical trends.

VIII. Conclusion

This paper detailed the design, modelling and implementation process of the Oceanic Glider. This design was aimed at producing a functional autonomous underwater vehicle to be used for research purposes. Several models were generated, studied, analysed and their suitability was judged for this project. This project provided a respectable platform for future development. With this foundation, a more comprehensive automation system could be realized such that the Glider was suitable for implementation as a functional research platform.

Acknowledgment

The authors would like to thank the Defence Science and Technology Organisation (DSTO) for in-kind support to the Project.

The authors would also like to thank the Electronic and Mechanical Engineering Work shop staff at the School of Mechanical Engineering, the University of Adelaide. The authors acknowledge P. Schmidt for advice and support throughout the course of this project. The authors would also like to acknowledge Mr. Amir Parsa Anvar for his editing and editorial comments on this paper.

References

[1] Bender, A, Steinberg, D, Friedman, A &Williams, S 2006, 'Analysis of an Autonomous Underwater Glider'.
[2] Davis, R, Eriksen, C & Jones, C 2002, 'Autonomous Buoyancy-Driven Underwater Gliders'.
[3] Guo, C, Kato, N n.d., 'Mini Underwater Glider (MUG) for Education'.
[4] Yun, L, Bliault, A & Doo, J 2010, 'Longitudinal Force Balance and Trim', in Springer US, Boston, MA, pp. 95-115Engineering, Vol. 224, pp. 437-447.
[5] Zimmerman, R, Chadwell, CD & Kussat, NH 2005, 'Absolute Positioning of An Autonomous Underwater Vehicle Using GPS And Acoustic Measurements', *IEEE Journal of Oceanic Engineering*, vol. 30, no. 1, pp. 153-164.